Int. J. Electrochem. Sci., 13 **(2018)** 11323 – 11334, doi: 10.20964/2018.11.03

International Journal of
ELECTROCHEMICAL
SCIENCE
www.electrochemsci.org

Corrosion Behavior of Nitrided Ni_3Al Intermetallic Alloy in 0.5 M H_2SO_4

E. Tapia-Bahena[1], *H. Martinez*[2], *J. Porcayo-Calderon*[1,2], *J.G. Gonzalez-Rodriguez*[1,*], *L. Martinez-Gomez*[2,3]

[1] Universidad Autonoma del Estado de Morelos, CIICAp, Av. Universidad 1001, Col. Chamilpa, 62209-Cuernavaca, Mor., Mexico.
[2] Universidad Nacional Autonoma de Mexico, Instituto de Ciencias Fisicas, Av. Universidad S/N, Col. Chamilpa, 62209-Cuernavaca, Mor., Mexico.
[3] Corrosion y Protección, (CyP), Buffon 46, 11590 Mexico D.F., Mexico
[*]E-mail: ggonzalez@uaem.mx

Received: 4 June 2018 / *Accepted:* 8 August 2018 / *Published:* 1 October 2018

The effect of plasma nitriding on the corrosion behavior of Ni_3Al intermetallic alloy in 0.5 M H_2SO_4 solution at 60 ^{0}C has been investigated by using potentiodynamic polarization curves, electrochemical impedance spectroscopy (EIS) and linear polarization resistance (LPR) measurements. Specimens were plasma nitrided at 500 and 600^{0}C during 8, 16 and 24 hours and were characterized by x-ray diffraction and scanning electronic microscopy. Results have shown that the thickness of nitride layer increased with nitriding time and temperature. Passive film properties were improved by nitriding. The corrosion resistance of nitride specimens increased with an increase either in the nitriding time or temperature. Specimens were susceptible to both uniform and localized types of corrosion.

Keywords: Ni_3Al, nitriding, acid corrosion.

1. INTRODUCTION

Due to their ability to develop an Al_2O_3 protective layer which provides corrosion resistance NiAl and Ni_3Al type intermetallics are widely used for their high temperature oxidation resistance [1-3]. However, their poor ductility is one of the main drawbacks. Despite that their main characteristic is high temperature corrosion resistance, these compounds are receiving attention as possible candidates to be used in other environments such as acidic, basic, chloride and sulfur-compound solutions [4-6]. This gives them the potential use in many industrial applications such as heat exchangers, where there

is the formation of sulfuric acid at temperatures between 60-120°C, in turbine blades, as biomaterials or as surgical instruments which are in contact with physiological fluids [7-10].

Nitriding is a widely employed surface treatment methodology which involves the introduction of nitrogen and results in improved wear and corrosion resistance as well as higher mechanical properties [11-22]. Thus, Zhang et al. [14] evaluated the corrosion resistance of plasma gas nitride nanocrystalline Inconel 718, finding that both wear and corrosion resistance properties were improved. In a similar work [15], Lee et al. evaluated a pre-oxidized and nitrided a 430 type stainless steel in a plasma gas, finding that its corrosion resistance and wear properties in 0.5 M H_2SO_4 solution were improved with these surface treatments. Li et al. [16] evaluated the wear and corrosion properties of an active screen plasma nitride 420 type stainless steel in a temperature range from 440 to 520^0C. They found that the nitrides layer thickness increased with increasing the temperature improving its wear resistance, hardness and corrosion resistance. Alphonsa et al. [17] improved the wear and corrosion resistance of 2205 duplex stainless steel by nitriding and nitro-carburizing it in a plasma gas in temperatures ranging from 350 to 500^0C during 4 hours, finding that the best properties were reached by treating the steel at 400^0C, decreasing these properties by increasing treating temperature. Thus, the goal of this work, is to evaluate the effect of plasma gas nitriding Ni_3Al intermetallic alloy on its corrosion behavior in 0.5 M H_2SO_4 solution, typically found in a many environment.

2. EXPERIMENTAL PROCEDURE

2.1 Testing material

Intermetallic Ni_3Al alloys were melted in an induction furnace using silicon carbide crucibles in an inert atmosphere. All elements were 99.9 % of purity. Specimens measuring 10 x 5 x 3 mm were prepared, polished with 3.0 μm alumina paste, washed and rinsed with acetone. They were nitride using a plasma with nitrogen gas using a pressure of 1 Torr, a current of 50 and 75 mA, equivalent to a temperature of 500 and 600 0C respectively, during 8, 16 and 24 hours. After this, they were encapsulated in commercial polymeric resin, abraded with 1200 grade emery paper, and rinsed with acetone. They were analyzed in a Scanning electronic microscope (SEM). X-ray diffraction patterns were performed by using a D2 Phaser, Bruker equipment with a Cu K_α radiation (1.5406 x 10^{-10} m wavelength), operated at 30 kV/10 mA.

2.2 Testing solution

As a corrosive environment, 0.5 M H_2SO_4 solution, prepared with bi-distilled water, was used, at a temperature of 60^0C.

2.3 Electrochemical techniques.

Electrochemical techniques employed included open circuit potentials (OCP) readings, potentiodynamic polarization curves, linear polarization resistance, LPR, and electrochemical

impedance spectroscopy, EIS. A three electrodes glass cell was used for this by using a graphite rod and a saturated calomel electrode as auxiliary and reference electrodes respectively. Polarization curves were recorded starting 300 mV more cathodic then the free corrosion potential, E_{corr}, and finishing 800 mV more anodic at a constant sweep rate of 1 mV/s. LPR measurements were performed applying a small perturbation signal to the working electrode of ± 10 mV, taking readings every 60 minutes during 24 hours. A similar perturbation was applied in the EIS measurements, but in this case was using AC signals at the Ecorr value in the frequency range 100 000-0.001 Hz. All experiments were carried out using an Interface 1000 Gamry Potentiostat/Galvanostat analyzer.

3. RESULTS AND DISCUSSION

3.1 Surface characterization.

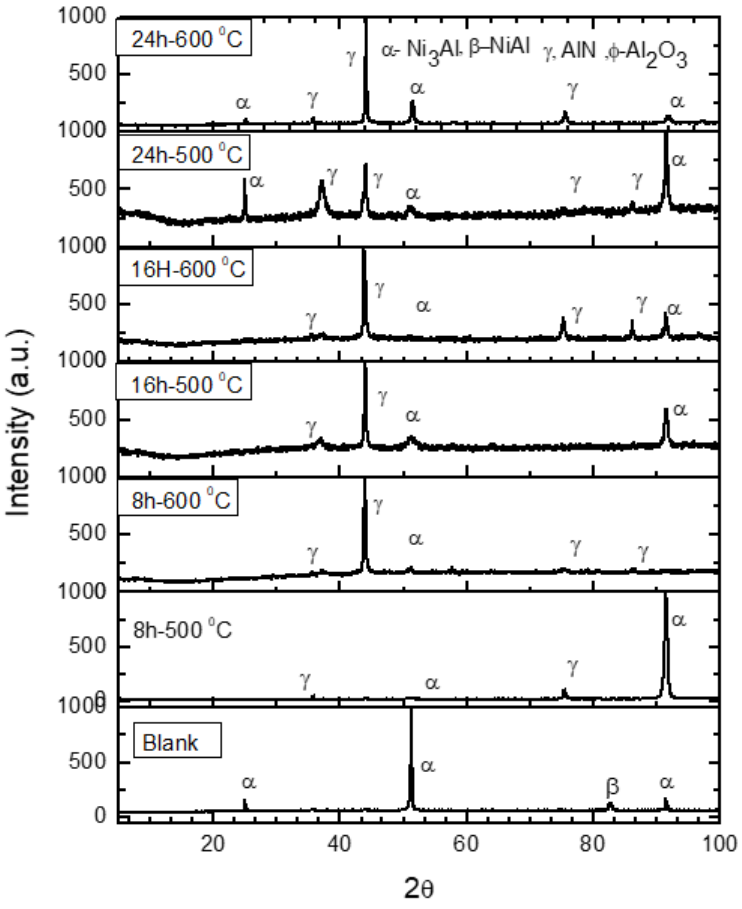

Figure 1. Effect of nitriding time and temperature on the X-ray patterns for Ni_3Al intermetallic alloy.

Compounds identified by the x-ray diffraction patterns for the different nitriding conditions, including for the specimen without nitriding treatment or blank, are given in Fig. 1. For the blank specimen, there were found only the Ni_3Al, base material, together with Al_2O_3 oxide, present on its surface. As soon as the specimen was nitride at 500^0C during 8 hours, the AlN phase was found in

addition to Ni_3Al, and Al_2O_3 phases. The intensity of the signal for the AlN phase increases with increasing both the nitriding time and temperature which is in agreement with reports from some other research works [16-18]. SEM micrographs of a cross section of the nitride specimens at 500 and 600 during 8 and 16 hours are shown in Fig. 2, where the nitride layer can be appreciated.

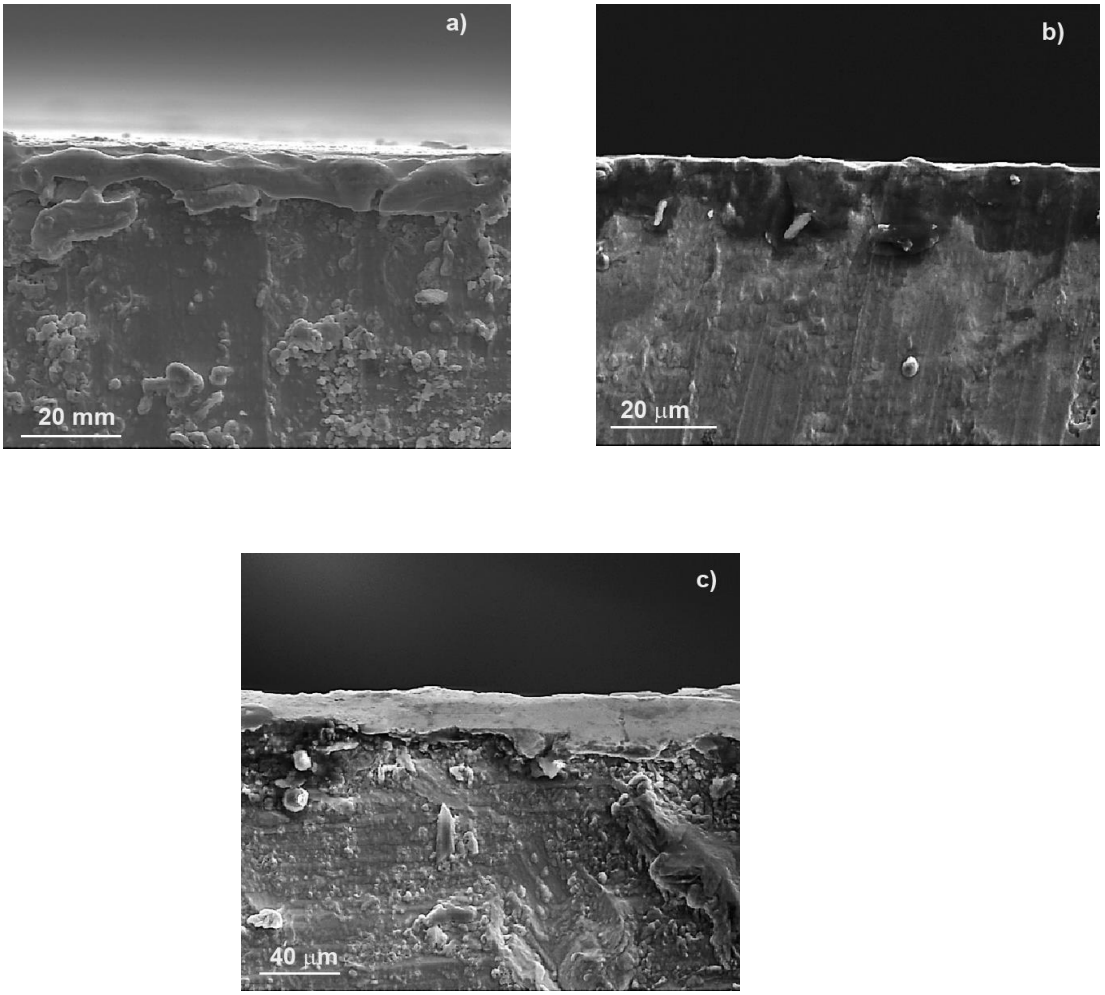

Figure 2. SEM micrograph of nitrided layers for Ni_3Al intermetallic alloy nitride at a) 600 ^{0}C, 8 hours, b) 500 ^{0}C, 16 hours, and c) 600 ^{0}C, 24 hours

Table 1. Variation on the nitride layer thickness with time and temperature.

Nitriding temperature (^{0}C)	Nitriding time (h)	Nitrided layer thickness (μm)
500	8	6
500	16	13
500	24	20
600	8	15
600	16	22
600	24	27

From the SEM pictures, the thickness of nitride layers were measured and they are given in table 1, which shows that this increases with an increase either in the nitriding time and temperature as reported by some other workers [16-18].

3.2 Open circuit potentials (OCP).

The effect of nitriding conditions on the variation of the OCP value with time in 0.5 M H_2SO_4 at 60 ^{0}C is given in Fig. 3.

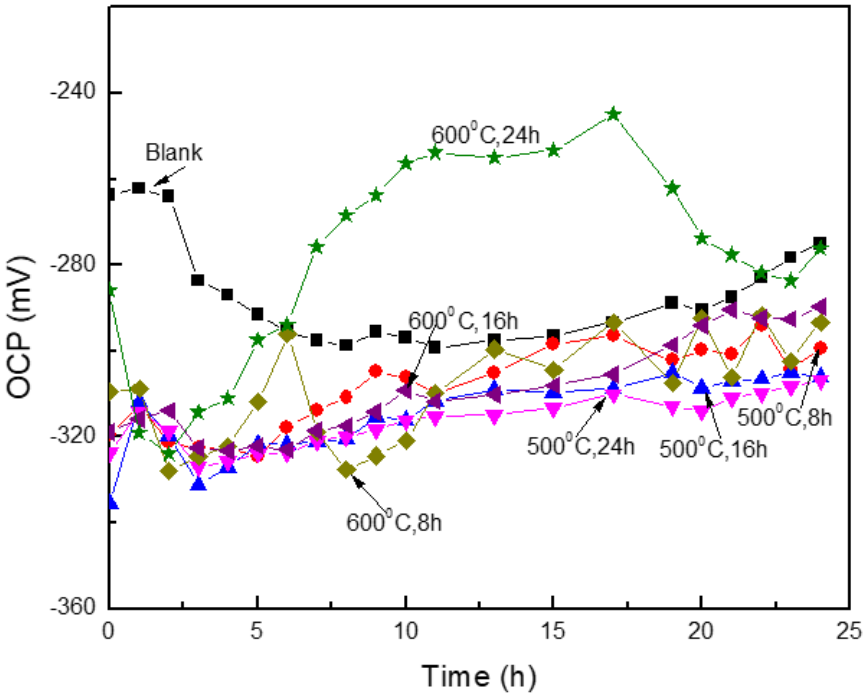

Figure 3. Effect of nitriding time and temperature on the OCP value for Ni_3Al intermetallic alloy in 0.5 M H_2SO_4 at at 60 ^{0}C.

It can be seen that the OCP value for the specimen without nitriding treatment was initially nobler than that for nitrided specimens. However, this value rapidly shifts towards more active values, decreasing from a value close to -260 mV down to -300 mV, and towards the end of the test, this value tends to shift towards nobler values. For nitrided specimens, the OCP value shifts slightly towards more active values during a few hours, but after this time it shifts towards nobler values and remains there during the whole testing time. When the OCP value is shifted towards more active values is because the metal/alloy is being corroded and dissolution of any pre-formed protective film is taking place, and when the shift of the OCP value is in the noble direction, is because the metal/alloy is covered by protective oxides film [23]. Thus, the shift of the OCP value for untreated specimen towards more active value corresponds to the dissolution of the pre-existing Al_2O_3 film by the electrolyte whereas the shift towards nobler values towards the end of the tests corresponds to the re-formation of this film. On the other hand, the shift of the OCP value of nitride specimens towards more active values at the beginning of the tests corresponds also to the dissolution of pre-formed Al_2O_3 film, but this sift was as not as significative as

for untreated specimen, indicating that any other protective film, like the AlN, was not dissolved, protecting the metal. After a few hours, the OCP value for nitride specimens shifted towards nobler values, indicating the formation of protective films.

3.3 Potentiodynamic polarization curves.

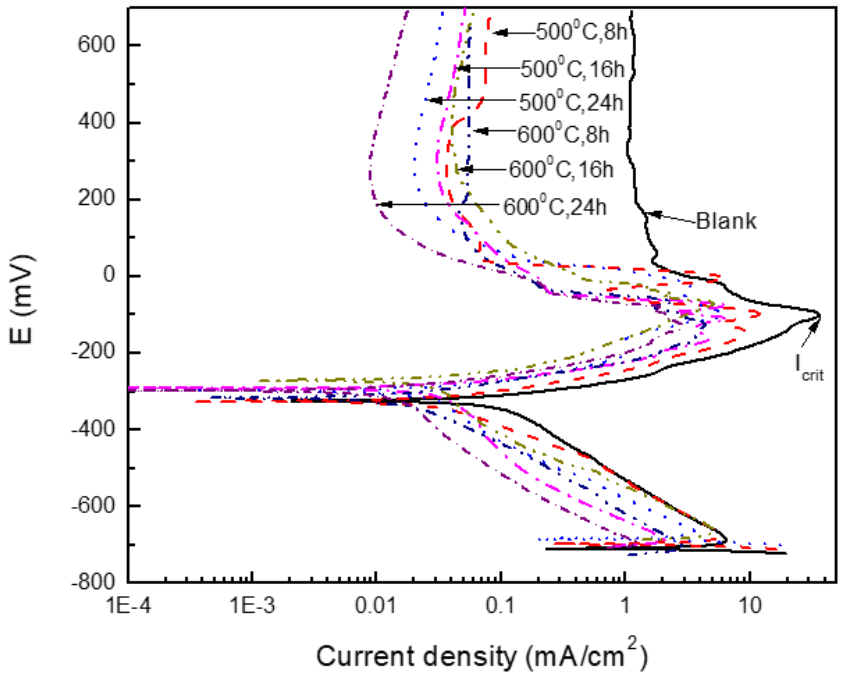

Figure 4. Effect of nitriding time and temperature on the polarization curves for Ni_3Al intermetallic alloy in 0.5 M H_2SO_4 at 60 ^{0}C.

Table 2. Electrochemical parameters obtained from polarization curves.

Nitriding temperature (^{0}C)	Nitriding time (h)	E_{corr} (mV)	I_{corr} (mA/cm^2)	I_{crit} (mA/cm^2)	I_{pas} (mA/cm^2)
blank	--	-325	0.09	34	1.05
500	8	-334	0.03	11.4	0.04
600	8	-270	0.03	6.2	0.035
500	16	-300	0.02	5.75	0.02
600	16	-320	0.02	5.15	0.015
500	24	-295	0.02	3.85	0.01
600	24	-300	0.01	2.28	0.007

The effect of nitriding time and temperature on the polarization curves for Ni3Al in 0.5 M H_2SO_4 at 60^{0}C is shown in Fig. 4. It can be seen that data describe an active-passive behavior, with an increase

in the anodic current density with the applied anodic potential until it reaches a critical current density value, I_{crit}, and then a decrease in the current density is observed giving place to a passive zone. The dissolution of the underlying alloy is the cause of this increase in the anodic current density and it reaches a critical value when the formation of an Al2O3 film starts [24]. When the dissolution of this protective layer takes place it is observed a new increase in the current density and Al is oxidised in to Al^{3+} ions [25]. Electrochemical parameters are given in table 2.

The highest I_{crit} value was for the untreated intermetallic alloy and it decreased with increasing either the nitriding time or temperature, obtaining its lowest value for specimen nitride at 600 ^{0}C during 24 hours. Additionally, both the passive current density, I_{pas}, and I_{corr} values decreased with increasing the nitriding time and temperature. Thus, the nitride layer improves the properties of the formed passive film by forming a film with better protecting properties for the underlying alloy form corrosion. The cathodic current density due to hydrogen evolution and oxygen reduction reactions are decreased with an increase in the nitriding time and temperature also. Thus, it is clear the beneficial effect of Al_2O_3 film to protect alloy, but it is necessary the formation of the nitride layer to protect Ni_3Al intermetallic alloy from further corrosion.

3.4 Linear polarization resistance measurements.

The effect of nitriding time and temperature on the variation of the polarization resistance value, R_p, with time is given in Fig. 5. In this figure it can be seen that the R_p value for nitride specimens were higher than those for untreated alloy. Th lowest R_p value, and thus the highest corrosion rate, corresponds to the blank specimen, with a value slightly lower than 100 ohm cm^2 which remained more or less constant during the whole testing time.

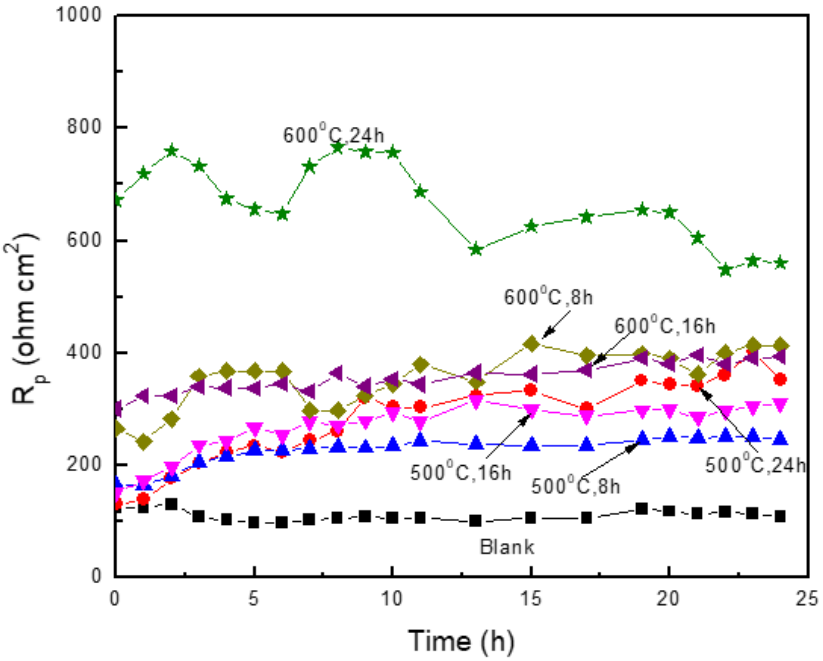

Figure 5. Effect of nitriding time and temperature on the R_p value for Ni_3Al intermetallic alloy in 0.5 M H_2SO_4 at 60 ^{0}C.

For nitrided specimens, the R_p value increased with an increase in either the nitriding time or temperature, which decreased, thus, the corrosion rate. For all the nitriding conditions, except at 600^0C during 24 hours, the R_p increased with an increase in the testing time, reaching a steady state value after a few hours. This increase in the R_p value, and thus a decrease in the corrosion rate, is due to the growth of a protective layer, which is mainly Al_2O_3 and AlN layers. Since the thickness of the AlN layer is constant for a given nitriding time and temperature, the increase in the R_p value is due to the growth of the Al_2O_3. On the other side, when the R_p value reaches a steady state value, is because this layer has reached a steady state thickness. For the specimen nitride at 600 ^{0}C during 24 hours, the R_p value decreases during some periods of time, but in some other periods in increases, due to the dissolution or breakdown of the Al_2O_3 layer and to its repair. The general trend of the R_p on these conditions is to decrease as testing time elapses, due to a uniform dissolution of the Al_2O_3 layer. In general terms, this figure shows that the corrosion rate of nitride Ni_3Al intermetallic alloy increases with an increase in the nitriding time or temperature.

3.5 EIS measurements.

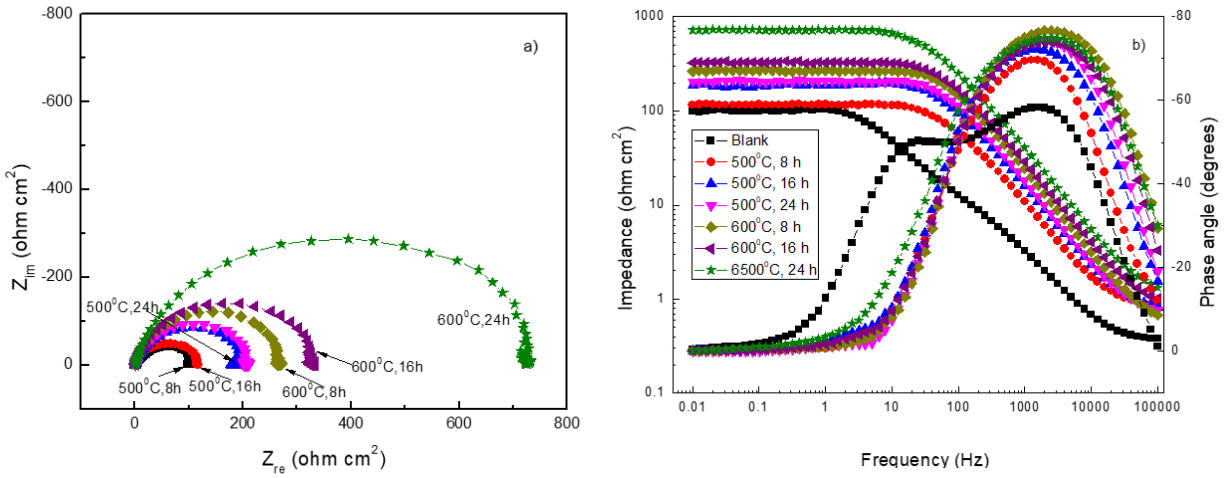

Figure 6. Effect of nitriding time and temperature on the EIS data in the a) Nyquist and b) Bode formats for Ni_3Al intermetallic alloy in 0.5 M H_2SO_4 at 60 ^{0}C.

EIS data in the Nyquist and Bode format for Ni_3Al with and without nitriding treatment are given in Fig. 6. Nyquist data, Fig. 6 a, shows only one capacitive loop, at all the frequency values, indicating that the corrosion process is under charge transfer control. The shape of the semicircle remained unaltered regardless of the nitriding time or the temperature, suggesting that the corrosion mechanism remained the same just as reported by other researchers [18]. The lowest semicircle diameter corresponds to the specimen without nitriding treatment, and it increased with an increase in the nitriding time or temperature. Bode diagrams, on the other hand, Fig. 6 b, indicates that the impedance or modulus increases with an increase in either the nitriding time or temperature and it reaches its highest value when specimen was nitrided at 600 ^{0}C during 24 hours. The shape of middle frequency linear part was very similar for untreated or treated specimens. The phase angle plot show two peaks for the untreated

specimen, indicating, thus, two phase constants, which corresponds to the double electrochemical layer and to the Al_2O_3 layer respectively. The presence of two phase constants was not very clear for the nitride specimens, however, the phase angle increased with an increase in the nitriding time or temperature, reaching a maximum value of -80 degrees for specimen nitrided at 600 ^{0}C during 24 hours.

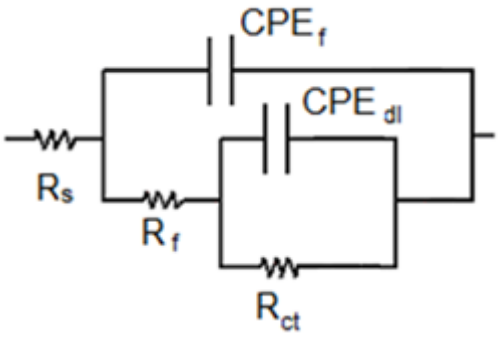

Figure 7. Equivalent electric circuit used to simulate EIS data.

EIS data were simulated by the electric circuit used in Fig. 7 where R_S is the solution resistance, R_{ct} the charge transfer resistance, R_f the resistance of the passive layer. Since the capacitive semicircles are depressed, CPE_{dl} and CPE_f are constant phase elements which have replaced ideal capacitances of the double layer and the passive layer respectively due to heterogeneities on the surface such as roughness due to corrosion, etc. [26, 27]. The impedance of a CPE is described by the expression:

$$Z_{CPE} = Y^{-1} (iw)^{-n} \quad (1)$$

where *Y* is the admittance, i is $\sqrt{-1}$, *w* is $2\pi f$, *f* the frequency and n is a parameter that gives surface properties such as roughness etc. Parameters obtained from the fitting impedance data are given in table 3.

Table 3. Electrochemical parameters used to simulate EIS data.

Nitriding conditions	R_s (ohm cm^2)	R_{ct} (ohm cm^2)	CPE_{dl} (μF cm^{-2})	n_{dl}	R_f (ohm cm^2)	CPE_f (μF cm^{-2})	n_f
blank	0.36	14	0.00017	0.85	93	0.00041	0.73
500^{0}C, 8h	0.78	11	4.86E-05	0.86	103	3.84E-5	0.76
500^{0}C,16h	0.74	15	2.94E-05	0.87	190	1.27E-5	0.81
500^{0}C, 24h	0.67	18	2.03E-05	0.90	198	9.23E-6	0.87
600^{0}C, 8h	0.53	21	1.49E-05	0.90	255	7.45E-6	0.79
600^{0}C,16h	0.82	27	1.51E-05	0.88	315	5.74E-6	0.85
600^{0}C, 24h	0.97	34	1.25E-05	0.87	704	3.57E-6	0.93

It can be seen that the resistance of the passive layer, R_f, is higher than that for R_{ct}, indicating that the corrosion resistance is dominated by the passive film resistance, which includes the Al_2O_3 and

AlN layers. In addition to this, R_{ct} does not change significantly by changing neither the nitriding time nor temperature, whereas R_f increases by modifying these parameters in accordance with the polarization curves results. Thus, R_f increases by increasing the nitriding time or temperature, which is due to the formation of a nitride and Al_2O_3 layer which improve the alloy corrosion resistance. Additionally, the passive layer capacitance value can be calculated with equation:

$$C_f = \varepsilon\varepsilon_0 A/\delta \quad (2)$$

where ε is the passive layer dielectric constant, ε_0 the vacuum electrical permittivity, δ the passive layer thickness, and A the surface area [28, 29]. Since parameters such as ε, ε_0 and A remained constant, the only reason why the C_f value decreased is because the thickness of the passive layer increased. Finally, parameter n is related with the surface roughness, and when the corrosion rate is low, it makes that the metal surface has a low surface roughness, and that the n_f value gets close to 1; on the contrary, when there are high corrosion rates and the metal surface roughness is high, the n_f value is close to 0.5. Table 3 shows that the lowest n_f value, and thus a highest surface roughness, corresponds to the blank specimen, whereas the highest n_f value, and thus the lowest surface roughness, was exhibited by specimen nitride at 600 ^{0}C during 24 hours.

3.6 SEM micrographs.

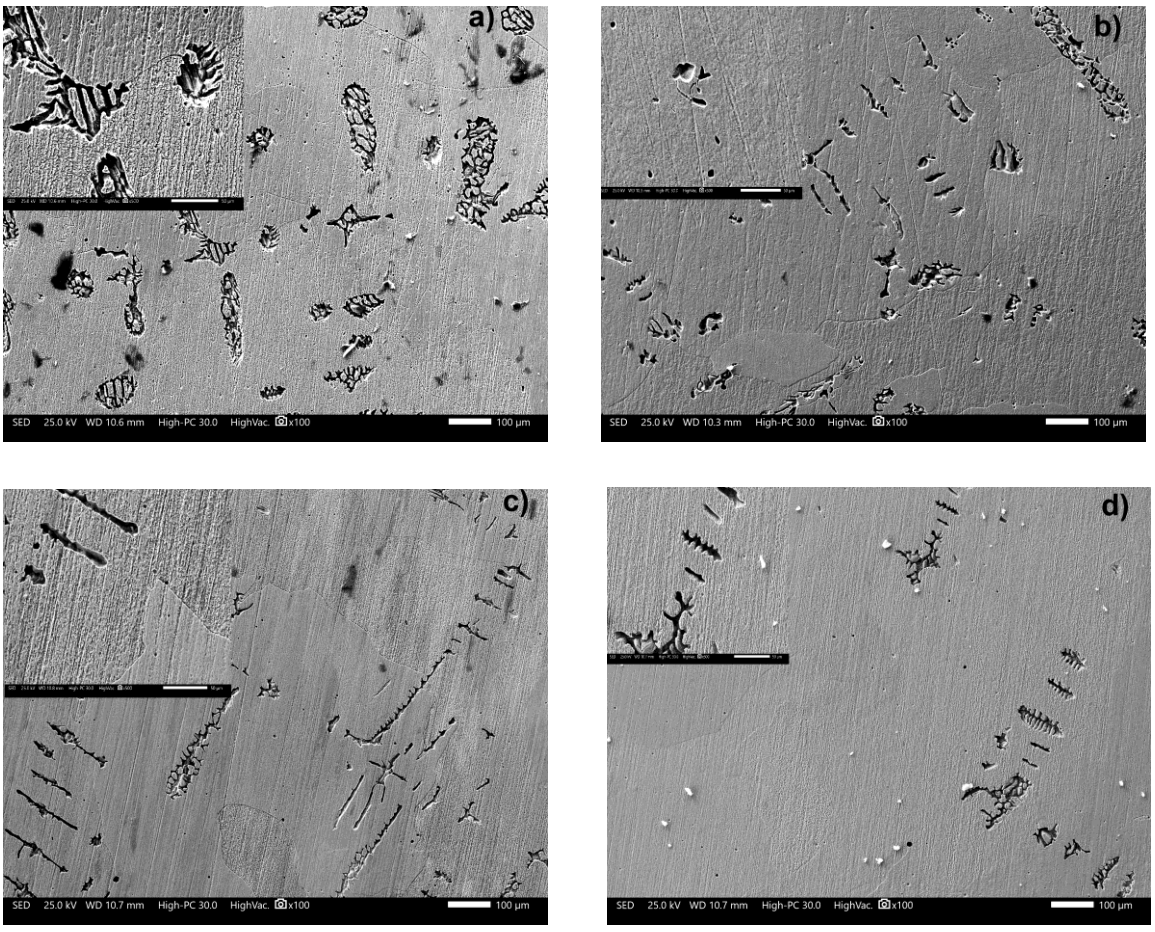

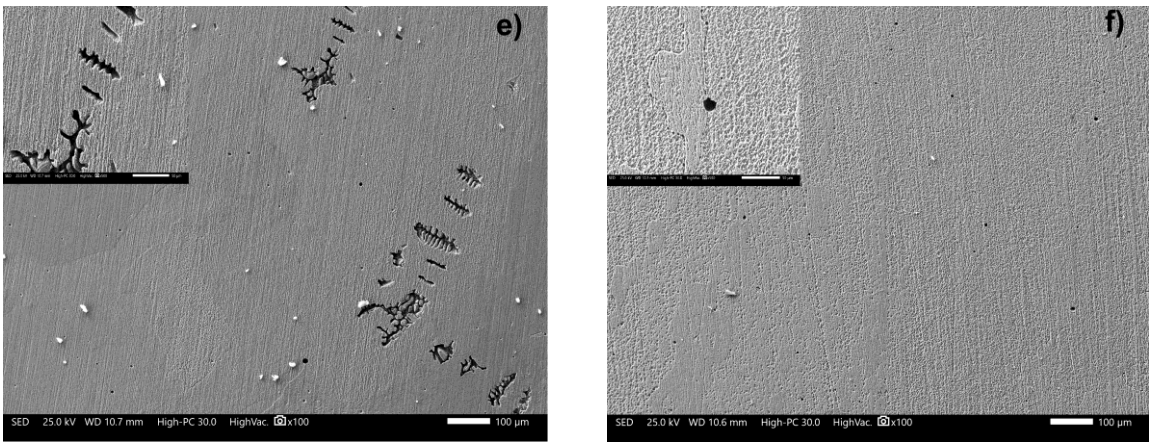

Figure 8. Micrograph of Ni_3Al intermetallic alloy nitride at a) 500 ^{0}C, 8 h, b) 600 ^{0}C, 8 h, c) 500 ^{0}C, 16 h, d) 600 ^{0}C, 16 h, e) 500 ^{0}C, 24 h, and e) 600 ^{0}C, 24 h, after corrosion tests in 0.5 M H_2SO_4 solution at 60 ^{0}C. Insert, the same specimen, at higher magnification.

Some SEM micrographs of corroded specimens after the LPR measurements are shown in Fig. 8. These figures show that specimens suffer from two types of corrosion, localized and uniform ones. In these pictures, some pits can be seen, which decrease in density with an increase either in the temperature or in the time of nitriding. These pits had a diameter between 5 and 10 µm. Another type of localized corrosion was observed on the specimens, which followed a dentritic-like pattern. The surface area covered by this type of corrosion decreased with an increase in the nitriding time or temperature. Thus, the most damaged material was the one nitride at 500 ^{0}C during 8 hours, whereas the least damaged was the one nitride at 600 ^{0}C during 24 hours, as reported in the electrochemical tests above. On the other hand, specimens suffered from a uniform type of corrosion which could be seen in the the surface roughness at higher magnifications. As explained above, a surface with a high dissolution rate shows a high roughness and a n_f value close to 1, which can be observed for specimens nitride at 500 or 600 ^{0}C during 8 hours, Figs. 7 a and b. On the other hand, specimens with a low dissolution rate, e.g. those nitrided at 500 or 600 ^{0}C during 24 hours exhibited a low surface roughness, with a n_f value close to 0.5 in accordance with data given in table 3.

4. CONCLUSIONS

A study of the corrosion resistance of plasma nitrided Ni_3Al intermetallic alloy in 0.5 M H_2SO_4 solution has been carried out. The thickness of the nitride layer increased with an increase either in the nitriding time or in temperature. Polarization curves showed that the passive film properties such as passivation and the critical current density values decreased by increasing either the time or temperature for nitriding. In addition to this, the corrosion resistance of nitride alloys increased either with increasing the nitriding time or temperature. EIS measurements have shown that the corrosion resistance of nitride alloys is due to their film resistance value. Specimens were susceptible to both uniform and localized type of corrosion such as pitting. The severity of corrosion damaged decreased by an increase either in the time or temperature for nitriding.

References

1. S.S. Parker, J. White, P. Hosemann and A. Nelson, *JOM,* 70 (2018) 186.
2. L. Zhu, G. Du, S. Bai, H. Zhang, Y. Ye and Y. Ai, *Corros. Sci.,* 123 (2017) 328.
3. E. Godlewska, M. Mitoraj and K. Leszczynska, *Corros. Sci.,* 78 (2014) 63.
4. A. Soleimani-Dorcheh and M. C. Galetz, *Oxid. Met*., 88 (2017) 549.
5. M.C. Garcia-Alonso, M.F. Lopez, M.L. Escudero, J.L. Gonzalez-Carrasco and D.G. Morris, *Intermetallics*, 7 (1999)185.
6. M. Negache, K. Taibi, N. Souami, H. Boucheme and R. Belkada , *Intermetallics*, 6 (2013) 73
7. G. Priyotomo, S. Wagle, K. Okitsu, A. Iwase, Y. Kaneno, R. Nishimura and T. Takasugi, *Corros. Sci*., 60 (2012)10.
8. C.T. Liu, J.O. Stiegler and FH. Fores , Metals Handbook, vol. 2. Metals Park, O.H.: ASM; 1990. 913.
9. G. Sharma, P.R. Singh, R.K. Gaonkar and R.V. Ramanujan, *J. Mater. Eng. Perf*. 16 (2007) 779.
10. R.V.Shankar, *Electrochim. Acta*, 49 (2004) 4533.
11. 11. H.J. Spies, C. Eckstein and H. Zimdars, *Surf. Eng.*, 18 (2002) 455.
12. D.Wen, *Surf. Coat. Technol.* 204 (2009) 511.
13. P. Novák, D. Vojtech and J.Serak, *Surf. Coat. Technol*., 200 (2006) 5229.
14. H. Zhang, H. Qin, Z. Ren, J. Zhao, X. Hou, G. Doll, Y. Dong and C. Ye, *Surf. Coat. Technol.,* 330 (2017)10.
15. S.H. Lee, T.H. Yang, S.H. Hyun and Y.S. Yoon, *Corros. Sci.,* 58 (2012) 79.
16. Y. Li, Y. He, J. Xiu, W. Wang, Y. Zhu and B. Hu, *Surf. Coat. Technol*., 329 (2017) 184.
17. J. Alphonsa, V.S. Raja and S. Mukherjee, *Corros. Sci*., 100 (2015) 121.
18. B.M. Girish, H.R. Vitala and M. Satis, *Corros. Eng. Sci. Technol.*, 48 (2012) 51.
19. C. Albayrak and A.A. Alsaran, *Corros. Eng. Sci. Technol.*, 49 (2013) 807.
20. J.C. Bryar, M.H. Jacobs and M.A. Ashworth, *Surf. Eng*., 16 (2000) 107.
21. M.T. Lin, C.H. Wan and W. Wu, *Int. J. Electrochem. Sci*., 9 (2014) 7832.
22. E. Ruiz, A. Delgado and W.Aperador, *Int. J. Electrochem. Sci*., 10 (2015) 9246.
23. K. Rahmouni, M. Keddam, A. Srhiri and H. Takenouti, *Corros. Sci*., 47 (2005) 3249.
24. M. Benmessaoud, K. Es-salah, N. Hajjaji, H. Takenouti, A. Srhiri and M. Ebentouhami, *Corros. Sci.,* 49 (2007) 3880.
25. K. Es-Salah, M. Keddam, K. Rahmouni, A. Srhiri and H. Takenouti, *Electrochim. Acta*, 49 (2004) 2771.
26. T. Poornima and J. Nayak, *Corros. Sci*., 53 (2011) 3688.
27. H. Keles, M. Keles, I. Dehri and O Serindag, *Mater. Chem. Phys.*, 112 (2008) 173.
28. E. Poorqasemi, O. Abootalebi, and M. Peikari, *Corros. Sci.,* 51 (2009)1043.
29. T. Poornima, J. Nayak and A.N. Shetty, *J. Appl. Electrochem*., 41 (2011) 223.